

Fig. 2.—Temperature vs. time in triple point (temperature of T_2O : Run 3).

diately after the preparation in order to minimize any small effects arising from tritium peroxide produced by the action of β -rays on the T_2O . The agreement of the three values, in spite of the presence of the material as liquid during part of the measurements, and the time lapse before the third determination, make it seem likely that such an effect is negligible. This conclusion is in accord with reasonable estimates of peroxide concentrations likely to exist, based on analyses of the decomposition gases of solid and liquid T_2O

made in other connections. In correcting the observations for the hydrogen content, the percentage tritium was assumed to be 99.35. This is an average of the original composition of the gas and the composition of gas collected later from the T_2O decomposition. The corresponding uncertainty in the triple point temperature amounts to 0.007° . From the above measurements, the triple point temperature of tritium oxide is taken to be $4.49 \pm 0.02^\circ$.

Prior to the measurements described above, a similar experiment was performed with deuterium, providing a test of the preparation system, particularly with regard to hydrogen contamination, as well as of the triple point apparatus. The preparation system was pretreated several times with deuterium. The triple point temperature was found to be 3.81° , in good agreement with the measurements of Taylor and Selwood² (3.82°), La Mer and Baker³ (3.80°), Bucken and Schäfer⁴ (3.80°), Long and Kemp⁵ (3.82°), and Stokland⁶ (3.813°).

The progressive increase of the triple point temperature in going from H_2O to T_2O is probably connected, at least in part, with an increasing strength of the hydrogen bonds in the solid, which is in turn to be associated with a decreasing zero point vibrational energy. This effect in the solid dominates over the oppositely acting effect in the liquid.

(2) H. S. Taylor and P. W. Selwood, *THIS JOURNAL*, **56**, 998 (1934).

(3) V. K. La Mer and W. N. Baker, *ibid.*, **56**, 2641 (1934).

(4) A. Eucken and K. Schäfer, *Ges. d. Wiss. Nachrichten. Math.-Phys. Kl. Fachgr. III. N.F. Bd.*, **1**, 109 (1935).

(5) E. A. Long and J. D. Kemp, *THIS JOURNAL*, **58**, 1829 (1936).

(6) K. Stokland, *Kgl. Norske. Videnskab. Selskabs, Forh.*, **10**, No. 39, 145 (1937); also *cf. C. A.*, **32**, 6121 (1938).

LOS ALAMOS, NEW MEXICO

[CONTRIBUTION FROM THE DEPARTMENT OF CHEMISTRY, YALE UNIVERSITY]

A General Theory for the Gouy Diffusion Method

BY LOUIS J. GOSTING^{1,2} AND LARS ONSAGER

RECEIVED APRIL 28, 1952

Equations are derived for the light intensity distribution and the positions of intensity zeros in a Gouy diffraction fringe pattern. This treatment goes beyond previous theory for the Gouy method by using a general mathematical approach and utilizing two different methods for integrating the wave optical amplitude equation. One procedure results in a series expansion which converges rapidly for the lower fringes while the other development yields an expression converging rapidly for the central fringes. By specializing the fringe minima relation to the case of ideal diffusion, additional terms are obtained (equation (62)) for the numerical factor, $(j + 3/4)$, in the interference condition of the original theory. Conditions which a cell mask must satisfy to minimize its disturbance of the Gouy fringes have been determined.

An experimental method for studying free diffusion in liquids, based on the Gouy interference phenomenon,^{3,4} has recently been developed and shown to be useful either for precision determinations⁵⁻⁷ or for rapid measurements.^{8,9} While the original theory for this method¹⁰ represented a good approximation to experimental conditions, its use of simple quadratic and cubic expressions to approximate the wave optical phase difference function did not allow accurate calculation of the relative fringe intensity distribution nor did it provide an estimate of the resulting error in the

fringe position equations. Both of these limitations are removed in the following development which by utilizing a general series expansion for the phase difference function yields series expansions for both the fringe system intensity and the fringe position equations. The relation of the previous theory to these expansions is indicated, and a comparison between them reveals that under certain conditions the latter must be used in order to obtain accurate diffusion coefficients. In addition, the following development is not restricted to Gaussian diffusion boundaries and may be applied to any non-Gaussian symmetrical boundaries or skew boundaries for which the phase difference function is known.

The Phase Function and Amplitude Equation

In the Gouy phenomenon monochromatic light of wave length λ from a horizontal source slit S, Fig. 1, is collimated by lens U_1 and focused by lens U_2 to form a slit image in plane P. The diffusion cell, C, when filled with homogeneous liquid of refractive index n_1 , Fig. 1a, has no effect on the

(1) du Pont Fellow, Yale University, 1949-1950.

(2) Department of Chemistry, University of Wisconsin, Madison, Wis.

(3) G. L. Gouy, *Compt. rend.*, **90**, 307 (1880).

(4) L. G. Longworth, *Ann. N. Y. Acad. Sci.*, **46**, 211 (1945).

(5) L. J. Gosting, E. M. Hanson, G. Kegeles and M. S. Morris, *Rev. Sci. Instruments*, **20**, 209 (1949).

(6) L. J. Gosting and M. S. Morris, *THIS JOURNAL*, **71**, 1998 (1949).

(7) L. J. Gosting, *ibid.*, **72**, 4418 (1950).

(8) C. A. Coulson, J. T. Cox, A. G. Ogston and J. St. L. Philpot, *Proc. Roy. Soc. (London)*, **A192**, 382 (1948).

(9) A. G. Ogston, *ibid.*, **A196**, 272 (1949).

(10) G. Kegeles and L. J. Gosting, *THIS JOURNAL*, **69**, 2516 (1947).

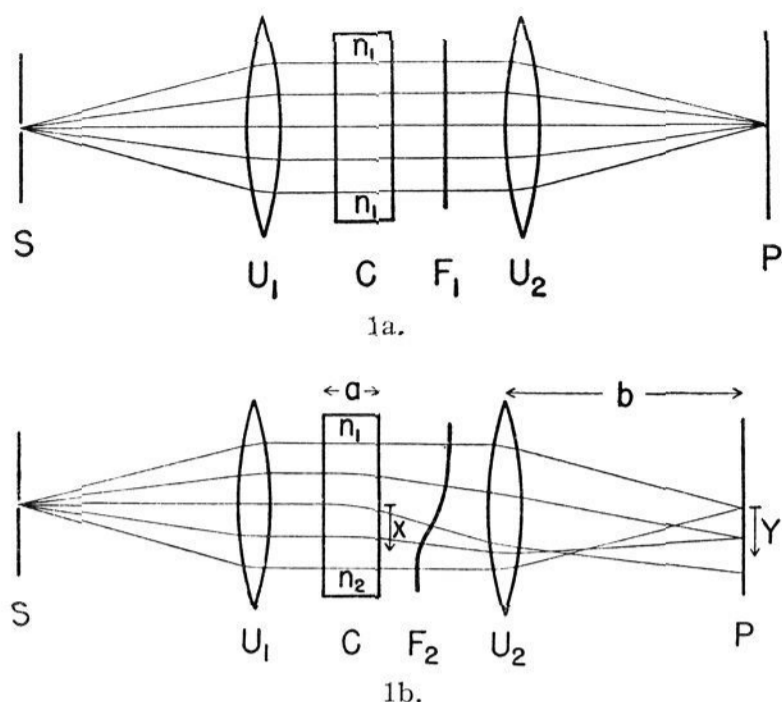


Fig. 1.—The Gouy diffusion apparatus showing (a) the straight wave front, F_1 , obtained when homogeneous liquid fills the diffusion cell, C, and (b) the distorted wave front, F_2 , resulting from a diffusing boundary in C.

shape of the wave front, F_1 , between the two lenses. With a freely diffusing boundary present between two regions of refractive index n_1 and n_2 , where $n_2 > n_1$, the wave front F_2 , Fig. 1b, is seen to suffer a non-uniform retardation. If the cell thickness, a , and the refractive index gradient are both reasonably small the magnitude of the retardation at a given level, x , is an where n , the refractive index of the solution, depends on both time and x . This deformation of the wave front produces interference fringes in plane P below the undeviated slit image, and their position likewise is a function of time.

At a given time, t , after formation of the initially sharp diffusion boundary, the light intensity, $I(Y)$, at a level Y below the slit image is given by¹¹

$$I(Y) = \psi\psi^* \quad (1)$$

where the amplitude, ψ , is obtained from

$$\psi = K \int e^{i\Phi(x)} g(x) dx \quad (2)$$

and its complex conjugate, ψ^* , is obtained by replacing i in this relation by $-i$. Since $e^{-i\Phi(x)} = \cos \Phi(x) - i \sin \Phi(x)$, it will be noted that apart from differences in notation this relation for ψ^* is equivalent to equation (17) of the previous theory¹⁰ except for the addition of a cell masking function, $g(x)$. Only for the special case of a symmetrical boundary, with symmetrical masking, is ψ^* equal to ψ . The proportionality constant, K , in equation (2) will not be further determined, and the integrals are taken over the entire wave front. The origin of x is taken at the level where dn/dx is a maximum, and similarly the phase difference function, $\Phi(x)$, is defined relative to a path through the maximum gradient of n , where $n = n_m$. This convention allows the equations to apply conveniently to skew, as well as symmetrical, bound-

aries. Adding phase differences due to the solution and air paths, we obtain

$$\Phi(x) = (2\pi/\lambda)[a(n - n_m) - x \sin(\arctan Y/b)] \quad (3)$$

or

$$\Phi(x) = (2\pi/\lambda)[a(n - n_m) - xY/b] \quad (4)$$

with reasonable precision when $Y/b < 0.01$, where the optical distance, b , is measured from the focal plane, P, to the nearer principal plane of lens U_2 . A small value of Y/b also ensures that ray bending in the cell will be small, so if a is also small n will be essentially constant over each light path through the cell as required by this form of the wave front retardation term.

The Path of Integration.—While $\Phi(x)$ is a real function in equation (4), its expansion into the complex plane, as illustrated by the Taylor expansion

$$\Phi(x + iy) = \Phi(x) + iy\Phi^I(x) - (1/2!)y^2\Phi^{II}(x) - (1/3!)iy^3\Phi^{III}(x) + \dots \quad (5)$$

is necessary for convenient integration of equation (2). The path of integration which will be followed in the x,y -plane between cell mask positions J_1 and J_2 is shown in Fig. 2. Associating subscripts 1 and 2 with negative and positive values of x , respectively, there will be two saddle points,¹² S_1 and S_2 , at values of x determined by $\Phi^I(x) = 0$, for every value of Y in the range $0 < Y < C_i = ab(dn/dx)_{\max}$. Since normals to the wave front at these levels will be focused at Y by lens L_2 , it follows that light traversing the cell at the level of a saddle point will contribute most to the amplitude at Y . Integration of equation (2) along paths B_1 and B_2 over these saddle points provides the contributions, ψ_{B_1} and ψ_{B_2} , of the diffusion boundary to the amplitude at Y . For these integrations the masking function, $g(x)$, of equation (2) is set equal to unity since the positions of closest masking, L_1 and L_2 , are assumed to be beyond the boundary in the region where dn/dx is essentially equal to zero. Since the integrand becomes nearly zero in the valleys, which are shown as shaded regions, into which paths B_1 and B_2 descend, the exact path of the dotted line connecting them is unimportant.

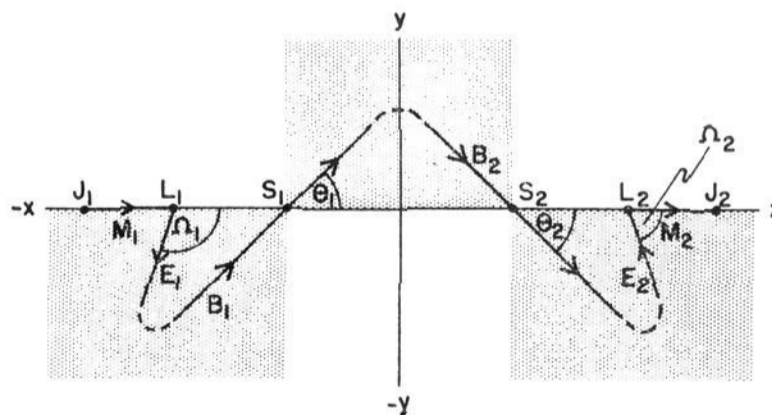


Fig. 2.—The path of integration between cell mask positions J_1 and J_2 in the complex plane (x,y).

When horizontal straight-edged masks are placed at levels L_1 and L_2 their contributions, ψ_{E_1} and ψ_{E_2} , to the amplitude are obtained by integrating along paths E_1 and E_2 from the mask positions into the valleys where, as before, the integrand is nearly

(11) J. C. Slater and N. H. Frank, "Introduction to Theoretical Physics," McGraw-Hill Book Co., New York, N. Y., 1933, p. 311; G. Joos, "Theoretical Physics," Hafner Publishing Co., New York, N. Y., 1934, p. 363 ff.

(12) H. Jeffreys and B. S. Jeffreys, "Methods of Mathematical Physics," Cambridge University Press, Cambridge, 1950, p. 503.

zero and connections to B₁ and B₂ may be made along any convenient path. Along paths E₁ and E₂ g(x) is set equal to unity, but along the x axis beyond L₁ and L₂ g(x) must equal zero since in this case all light is cut off by the mask and the total amplitude at level Y becomes ψ_{E₁} + ψ_{B₁} + ψ_{B₂} + ψ_{E₂}.

Other masking cases may be considered by letting g(x) equal zero only when x < J₁ and x > J₂ and designing the mask so g(x) decreases from unity to zero between L₂ and J₂ and between L₁ and J₁. Then the contributions ψ_{M₁} and ψ_{M₂} for paths M₁ and M₂ do not equal zero and must be included. Requirements which g(x) must satisfy in this region if disturbances of the Gouy fringes by the cell mask are to be minimized will be discussed below in a section on masking.

The Phase Function for Ideal Diffusion.—To obtain a complete solution of equation (2) n must be expressed as a function of x in equation (4). Following the notation of the original theory¹⁰ for a single solute which diffuses ideally, producing a Gaussian boundary, and assuming that the index of refraction of the solution varies linearly with the weight of solute per unit volume of solution

$$n = n_m + [(n_2 - n_1)/\sqrt{\pi}] \int_0^z e^{-\beta^2} d\beta \quad (6)$$

where

$$z = x/(2\sqrt{Dt}) \quad (7)$$

Here D represents the diffusion coefficient and t is time since formation of the initially sharp boundary between the two solutions. Defining the experimentally determined total number, j_m, of fringes by

$$j_m = a(n_2 - n_1)/\lambda \quad (8)$$

and

$$C_t = ab(dn/dx)_{\max} = j_m \lambda b/(2\sqrt{\pi}Dt) \quad (9)$$

the phase difference function, equation (4), for this case becomes

$$\Phi(x) = \varphi(z) = 2\sqrt{\pi}j_m \left[\int_0^z e^{-\beta^2} d\beta - zY/C_t \right] \quad (10)$$

An examination of the maxima of equations (4) and (10) indicates that, for any boundary, at a given time C_t is the greatest downward displacement of light in the focal plane, P, predicted by geometrical optics.

Although the above derivation has been for the case of collimated light through the diffusion cell, the phase difference function represented by equation (10) also applies to the case where lens U₂ is omitted and a single long focus lens at the position of U₁ is used to focus the source slit.¹⁰ In the single lens apparatus, however, the boundary should be located on the optic axis and b is measured from the focal plane to the center of the diffusion cell.

The problem is to solve equations (2) and (10) for C_t in terms of the downward displacement, Y_j, of any fringe numbered j, since when C_t is known the diffusion coefficient, D, may be evaluated from equation (9). Here j = 0, 1, 2, . . . with the lowest fringe assigned the number zero. The interference condition derived for intensity zeros in the original theory¹⁰ was

$$(j + 3/4)/j_m = f(z_j) = (2/\sqrt{\pi}) \left[\int_0^{z_j} e^{-\beta^2} d\beta - z_j e^{-z_j^2} \right] \quad (11)$$

where z_j denotes the value of z for fringe numbered j. After determining f(z_j) from j and j_m, the corresponding value of e^{-z_j²} was obtained from a table of e^{-z²} versus f(z_j) and C_t calculated from the relation

$$Y_j/C_t = e^{-z_j^2} \quad (12)$$

which is derived by setting the first derivative of equation (10) equal to zero. One result of the present work is the derivation of correction terms for (j + 3/4) in equation (11).

Integration of the Amplitude Equation for the Diffusion Boundary

The following integration procedures allow the computation of the amplitude and the interference conditions whenever the phase function, Φ(x), is known. In some experimental cases equation (10), or even equation (4), may not be sufficiently accurate; for example, the assumption that n is linear with the solute concentration may be poor or a may be so large that n changes appreciably over a given path through the cell. Correct results may then be obtained by applying the following integration procedures to the corrected phase function.

Expansion in Airy Integrals.—Before solving equation (2) by integrating over the saddle points indicated in Fig. 2, an alternative method of solution will be presented. A general approach would be possible by expanding the phase function, Φ(x), as a Taylor series about the origin and then writing equation (2) as a series in the Airy integral and its derivatives. This procedure is useful for only the lower fringes, however, and only the special case of ideal diffusion will be treated by this method.

Expanding equation (10) as a power series in z, and substituting

$$\epsilon = (2\sqrt{\pi}j_m)^{2/3} \quad (13)$$

$$\alpha = \epsilon[(Y/C_t) - 1] \quad (14)$$

and

$$u = z\epsilon^{1/2} \quad (15)$$

the contribution of the diffusing boundary to the amplitude, equation (2) may be written

$$\psi_B = 2\sqrt{(Dt/\epsilon)} K \int e^{-i(\alpha u + \frac{1}{3}u^3)} e^{-i(-\frac{u^5}{10\epsilon} + \frac{u^7}{42\epsilon^2} - \frac{u^9}{216\epsilon^3} + \dots)} du \quad (16)$$

Expanding the second exponential as a series, deforming the path of integration up to the x-axis, and defining the Airy integral by

$$Ai(\alpha) = [1/(2\pi)] \int_{-\infty}^{\infty} e^{-i(\alpha u + \frac{1}{3}u^3)} du \quad (17)$$

so its derivatives become

$$Ai^m(\alpha) = [(-i^m)/(2\pi)] \int_{-\infty}^{\infty} u^m e^{-i(\alpha u + \frac{1}{3}u^3)} du \quad (18)$$

equation (16) reduces to the asymptotic expression

$$\psi_B = 4\pi K \sqrt{Dt/\epsilon} \left\{ Ai(\alpha) - \frac{Ai^V(\alpha)}{10\epsilon} - \frac{1}{\epsilon^2} \left[\frac{Ai^{VI}(\alpha)}{42} - \frac{Ai^X(\alpha)}{200} \right] - \frac{1}{\epsilon^3} \left[\frac{Ai^{IX}(\alpha)}{216} - \frac{Ai^{XII}(\alpha)}{420} + \frac{Ai^{XV}(\alpha)}{6000} \right] - \dots \right\} \quad (19)$$

Successive applications of the recursion formula

$$Ai^m(\alpha) = (m - 2)Ai^{m-3}(\alpha) + \alpha Ai^{m-2}(\alpha) \quad (20)$$

which may be derived from the differential equation

$$g^{II} = xg \quad (21)$$

satisfied by the Airy integral, provides the final expression for the amplitude. Substitution in equation (1) yields the intensity relation

$$I(Y) = (16\pi^2 K^2 D l / \epsilon) \left\{ Ai(\alpha) \left[1 - \frac{2\alpha}{5\epsilon} + \frac{1}{\epsilon^2} \left(\frac{2\alpha^2}{7} + \frac{\alpha^5}{200} \right) - \frac{1}{\epsilon^3} \left(\frac{47}{675} + \frac{2347\alpha^3}{9450} + \frac{81\alpha^6}{14000} \right) + \dots \right] + Ai^I(\alpha) \left[-\frac{\alpha^2}{10\epsilon} + \frac{1}{\epsilon^2} \left(\frac{17}{105} + \frac{8\alpha^3}{105} \right) - \frac{1}{\epsilon^3} \left(\frac{1223\alpha}{4725} + \frac{1163\alpha^4}{18900} + \frac{\alpha^7}{6000} \right) + \dots \right] \right\}^2 \quad (22)$$

for the lower fringes of a Gaussian boundary when diffraction from the cell mask is neglected.

The interference condition for intensity zeros is obtained by replacing $Ai(\alpha)$ and $Ai^I(\alpha)$ by their Taylor expansions about α_j where α_j is defined by $Ai(\alpha_j) = 0$, and the new variable is denoted by

$$\xi = \alpha - \alpha_j \quad (23)$$

Setting the intensity equal to zero, eliminating derivatives of $Ai(\alpha)$ higher than the first by equation (20), and solving for ξ by successive approximations

$$\xi = \frac{\alpha_j^2}{10\epsilon} - \frac{17(10 + \alpha_j^2)}{1050\epsilon^2} + \frac{30560\alpha_j + 1019\alpha_j^4}{189000\epsilon^3} - \dots \quad (24)$$

Combining this result with equations (14) and (23) we have the interference condition provided by this Airy integral expansion

$$\frac{Y_j}{C_t} = 1 + \frac{\alpha_j}{\epsilon} + \frac{\alpha_j^2}{10\epsilon^2} - \frac{17(10 + \alpha_j^2)}{1050\epsilon^3} + \frac{1019[(30560/1019)\alpha_j + \alpha_j^4]}{189000\epsilon^4} - \dots \quad (25)$$

where Y_j denotes values of Y for the j th intensity zeros. Using an approximate coefficient for α_j in the fifth term and replacing ϵ by j_m according to equation (13)

$$\frac{Y_j}{C_t} = 1 + 0.430127 \frac{\alpha_j}{(j_m)^{2/3}} + 0.018501 \frac{\alpha_j^2}{(j_m)^{4/3}} - 0.001288 \frac{(10 + \alpha_j^2)}{(j_m)^{5/3}} + 0.000185 \frac{(30\alpha_j + \alpha_j^4)}{(j_m)^{8/3}} - \dots \quad (26)$$

Solutions of this equation are readily obtained using the roots, α_j , of the Airy integral. The first 50 roots have been tabulated to eight decimal places and published by the British Association.¹³ Approximate values for the first five roots are given in Table I so the relative magnitude of the terms in equation (26) may be readily observed. Values of

TABLE I
ROOTS OF THE AIRY INTEGRAL

j	0	1	2	3	4
α_j	-2.338	-4.088	-5.521	-6.787	-7.944

D are then computed from equation (9) by inserting C_t from equation (26), subject to the possible neces-

sity of extrapolating to $1/t = 0$ if the initial boundary was not sufficiently sharp.¹⁴

Integration by Method of Steepest Descents.— Since the minimum and maximum of equation (4) become saddle points (Fig. 2) for the integrand, $e^{i\Phi(x)}$, when $\Phi(x)$ is expanded into the complex plane, asymptotic solutions of equation (2) may be derived by the method of steepest descents¹² when Y lies in the range $0 < Y < C_t = ab(dn/dx)_{\max}$. First, a general solution for the amplitude will be obtained which is valid for any phase difference function for diffusion, $\Phi(x)$; then the results will be specialized to the case of a Gaussian boundary.

Using subscripts 1 and 2 to identify the following quantities with the minima or maxima, respectively, of $\Phi(x)$, denoting the modulus about these points by ζ , and setting $g(x) = 1$, the contribution of the diffusion boundary to equation (2) becomes

$$\psi_B = \psi_{B_1} + \psi_{B_2} = K \sum_{k=1,2} \int_{-\infty}^{\infty} \exp[i\Phi(x_k + e^{i\theta} \zeta)] (e^{i\theta} \zeta) d\zeta \quad (27)$$

where θ is the polar coordinate, to be assigned a convenient value later, measured counter-clockwise from the positive direction of x . Expanding $\Phi()$ as a Taylor series about x_k , and remembering that $\Phi^I(x_1) = \Phi^I(x_2) = 0$, either integral of equation (27) may be written

$$\psi_{B_k} = K e^{i[\Phi(x_k) + \theta_k]} \int_{-\infty}^{\infty} \exp i \left\{ [\Phi^{II}(x_k) e^{2i\theta} \zeta^2 / 2] + \sum_{m=3}^{\infty} [\Phi^m(x_k) e^{mi\theta} \zeta^m / m!] \right\} d\zeta \quad (28)$$

While this integral could be evaluated by expanding $\exp i \sum_{m=3}^{\infty}$ as a power series in ζ , it is more convenient to obtain an automatic grouping of terms according to inverse powers of j_m by the following method. Defining v by

$$\Phi^{II}(x_k) e^{2i\theta} \zeta^2 / 2 = \left\{ [\Phi^{II}(x_k) e^{2i\theta} \zeta^2 / 2] + \sum_{m=3}^{\infty} [\Phi^m(x_k) e^{mi\theta} \zeta^m / m!] \right\} \quad (29)$$

we may write

$$\zeta = v / \sqrt{p_k} \quad (30)$$

where

$$p_k = \left\{ 1 + [2e^{-2i\theta_k / \Phi^I(x_k)}] \sum_{m=3}^{\infty} [\Phi^m(x_k) e^{mi\theta} \zeta^{m-2} / m!] \right\} \quad (31)$$

Lagrange's method for inverting a series¹⁵ then gives

$$\zeta = \sum_{r=1}^{\infty} \frac{v^r}{r!} \frac{d^{r-1}}{d\zeta^{r-1}} [p_k^{-1/2}]_{\zeta=0} \quad (32)$$

and

$$d\zeta = \sum_{r=1}^{\infty} \frac{v^{r-1}}{(r-1)!} \frac{d^{r-1}}{d\zeta^{r-1}} [p_k^{-r/2}]_{\zeta=0} dv \quad (33)$$

(13) "The Airy Integral," British Association for the Advancement of Science Mathematical Tables, Part-Volume B, University Press, Cambridge, 1946.

(14) L. G. Longworth, THIS JOURNAL, 69, 2510 (1947).

(15) Whittaker and Watson, "A Course of Modern Analysis," Cambridge University Press, Cambridge, 1927, p. 133.

so equation (28) becomes

$$\psi_{B_k} = K e^{i[\Phi(x_k) + \theta_k]} \int_{-\infty}^{\infty} \{ \exp i[\Phi^{II}(x_k) e^{2i\theta_k} v^2/2] \} \times \sum_{r=1}^{\infty} \frac{v^{r-1}}{(r-1)!} \frac{d^{r-1}}{d\xi^{r-1}} [p_k^{-r/2}]_{\xi=0} dv \quad (34)$$

Since $\Phi^{II}(x_1) > 0$ and $\Phi^{II}(x_2) < 0$ it is seen that by assigning the values

$$\theta_1 = +\pi/4, \theta_2 = -\pi/4 \quad (35)$$

all terms in the series may be integrated by the relationship

$$\int_{-\infty}^{\infty} v^{r-1} e^{-cv^2} dv = \begin{cases} 0 & \text{if } r = 2, 4, 6, \dots \\ \frac{(r-1)! \sqrt{\pi/c}}{[(r-1)/2]! (4c)^{(r-1)/2}} & \text{if } r = 1, 3, 5, \dots \end{cases} \quad (36)$$

Substituting

$$r-1 = 2s \quad s = 0, 1, 2, \dots \quad (37)$$

equation (34) becomes

$$\psi_{B_k} = K e^{i[\Phi(x_k) + \theta_k]} \left[\frac{2\pi}{(-1)^{k-1} \Phi^{II}(x_k)} \right]^{1/2} \times \sum_{s=0}^{\infty} \frac{1}{2^s (s!) [(-1)^{k-1} \Phi^{II}(x_k)]^s} \frac{d^{2s}}{d\xi^{2s}} [p_k^{-(s+1/2)}]_{\xi=0} \quad (38)$$

After solving for the derivatives of $p_k^{-(s+1/2)}$, the expression

$$\psi_{B_k}/K = e^{i[\Phi(x_k) + \pi/4]} (V_1 + iW_1) + e^{i[\Phi(x_k) - \pi/4]} (V_2 + iW_2) \quad (39)$$

is obtained for the amplitude where¹⁶

$$V_k = \left[\frac{2\pi}{(-1)^{k-1} \Phi^{II}} \right]^{1/2} \left\{ 1 - \frac{385}{1152} \frac{1}{(\Phi^{II})^2} \left[\left(\frac{\Phi^{III}}{\Phi^{II}} \right)^4 - \frac{18}{11} \frac{(\Phi^{III})^2 \Phi^{IV}}{(\Phi^{II})^3} + \frac{3}{11} \left(\frac{\Phi^{IV}}{\Phi^{II}} \right)^2 + \frac{24}{55} \frac{\Phi^{III} \Phi^V}{(\Phi^{II})^2} - \frac{24}{385} \frac{\Phi^{VI}}{\Phi^{II}} \right] + \dots \right\} \quad (40)$$

and

$$W_k = \left[\frac{2\pi}{(-1)^{k-1} \Phi^{II}} \right]^{1/2} \left\{ + \frac{5}{24} \frac{1}{\Phi^{II}} \left[\left(\frac{\Phi^{III}}{\Phi^{II}} \right)^2 - \frac{3}{5} \frac{\Phi^{IV}}{\Phi^{II}} \right] - \frac{85085}{82944} \frac{1}{(\Phi^{II})^3} \left[\left(\frac{\Phi^{III}}{\Phi^{II}} \right)^6 - \frac{45}{17} \frac{(\Phi^{III})^4 \Phi^{IV}}{(\Phi^{II})^3} + \frac{27}{17} \frac{(\Phi^{III})^2 (\Phi^{IV})^2}{(\Phi^{II})^4} + \frac{72}{85} \frac{(\Phi^{III})^3 \Phi^V}{(\Phi^{II})^4} - \frac{27}{221} \left(\frac{\Phi^{IV}}{\Phi^{II}} \right)^3 - \frac{648}{1105} \frac{\Phi^{III} \Phi^{IV} \Phi^V}{(\Phi^{II})^3} - \frac{216}{1105} \frac{(\Phi^{III})^2 \Phi^{VI}}{(\Phi^{II})^3} + \frac{1944}{60775} \left(\frac{\Phi^V}{\Phi^{II}} \right)^2 + \frac{648}{12155} \frac{\Phi^{IV} \Phi^{VI}}{(\Phi^{II})^2} + \frac{2592}{85085} \frac{\Phi^{III} \Phi^{VII}}{(\Phi^{II})^2} - \frac{216}{85085} \frac{\Phi^{VIII}}{\Phi^{II}} \right] + \dots \right\} \quad (41)$$

Defining

$$\gamma_k = \Phi(x_k) + \theta_k \quad (42)$$

the intensity, equation (1), for any diffusion boundary becomes

$$I(Y) = K^2 [V_1^2 + W_1^2 + V_2^2 + W_2^2 + 2[V_1 V_2 + W_1 W_2] \cos(\gamma_2 - \gamma_1) - 2[V_1 W_2 - W_1 V_2] \sin(\gamma_2 - \gamma_1)] \quad (43)$$

Imposing the restrictions that

$$\Phi^m(x_1) = -\Phi^m(x_2) \quad m = 0, 2, 4, \dots \quad (44)$$

and

$$\Phi^m(x_1) = \Phi^m(x_2) \quad m = 1, 3, 5, \dots \quad (45)$$

(16) To simplify the notation in equations (40) and (41) Φ^m is used to denote $\Phi^{mI}(x_k)$.

it is seen from equations (40) and (41) that $V_1 = V_2$ and $W_1 = -W_2$, so the intensity equation for any symmetrical diffusion boundary reduces to

$$I(Y) = 4K^2 [V_2 \cos \gamma_2 - W_2 \sin \gamma_2]^2 \quad (46)$$

Finally, consider a Gaussian boundary in which the refractive index is given by equation (6). Since

$$z_2 = x_2/(2\sqrt{Dt}) \quad (47)$$

simplification of equation (46) may now be obtained by substituting $\varphi^m(z_2)$ for $\Phi^m(x_2)$ according to the relation

$$\Phi^m(x_2) = (2\sqrt{Dt})^{-m} \varphi^m(z_2) \quad (48)$$

The factor $(2\sqrt{Dt})$ cancels out of all but the square root terms in V_2 and W_2 . The derivatives, $\varphi^m(z_2)$, where $m = 2, 3, 4, \dots$, are obtained by differentiation of equation (10), while γ_2 is determined by substituting the relation

$$Y/C_t = e^{-z^2} \quad (49)$$

for maxima in equation (10) back into that equation giving

$$\gamma_2 = \pi j_m f(z_2) - \pi/4 \quad (50)$$

The function $f(z)$ is defined as before by equation (11).

Defining z as positive so the subscripts, 2, may be dropped for convenience, the final expression for the fringe intensity for an ideal diffusion becomes

$$I(Y) = 4K^2 \{ V \cos[\pi j_m f(z) - \pi/4] - W \sin[\pi j_m f(z) - \pi/4] \}^2 \quad (51)$$

where

$$V = 2\sqrt{Dt} h^{-1/2} \left[1 - \frac{385}{4608} (\pi h z^2)^{-2} \sigma_2(z) + \dots \right] \quad (52)$$

$$W = 2\sqrt{Dt} h^{-1/2} \left[-\frac{5}{48} (\pi h z^2)^{-1} \sigma_1(z) + \frac{85085}{663552} (\pi h z^2)^{-3} \sigma_3(z) - \dots \right] \quad (53)$$

in which

$$h = (2/\sqrt{\pi}) z e^{-z^2} j_m \quad (54)$$

$$\sigma_1(z) = 1 - \frac{2}{5} z^2 + \frac{8}{5} z^4 \quad (55)$$

$$\sigma_2(z) = 1 - \frac{4}{5} z^2 - \frac{12}{385} z^4 + \frac{32}{35} z^6 + \frac{64}{385} z^8 \quad (56)$$

$$\sigma_3(z) = 1 - \frac{6}{5} z^2 + \frac{948}{1925} z^4 - \frac{4744}{425425} z^6 - \frac{8544}{425425} z^8 - \frac{20352}{425425} z^{10} - \frac{71168}{425425} z^{12} \quad (57)$$

The interference condition for zeros of intensity is obtained by setting $I(Y) = 0$ in equation (51) giving

$$\tan \pi [j_m f(z) - 1/4] = V/W \quad (58)$$

and expanding as an arctan series

$$\pi [j_m f(z) - 1/4] = (j + 1/2)\pi - (W/V) + \frac{(1/3)(W/V)^3}{\dots} \quad (59)$$

where $j = 0, 1, 2, \dots$. Defining

$$R(z) = (3\sqrt{\pi/4}) f(z) z^{-2} e^{z^2} = (3\pi/2) [j_m f(z)] / (\pi h z^2) \quad (60)$$

which approaches unity as z approaches zero, W/V may be written

$$\frac{W}{V} = -\frac{5}{72\pi} \frac{R(z) \sigma_1(z)}{[j_m f(z)]} + \frac{85085}{2239488\pi^3} \left[\frac{\sigma_3(z)}{\sigma_1(z) \sigma_2(z)} - \frac{1155}{17017} \frac{[R(z)]^2}{[j_m f(z)]^3} - \dots \right] \quad (61)$$

Substituting in equation (59) gives the final interference condition for the case of a single, ideally diffusing, solute

$$i_m f(z_j) = j + \frac{3}{4} + 0.0070362 \frac{G_1(z_j)}{[j_m f(z_j)]} - 0.00036471 \frac{G_2(z_j)}{[j_m f(z_j)]^3} + \dots \quad (62)$$

The subscript j has been added to denote the intensity zero numbered j , and

$$G_1(z_j) = R(z_j)\sigma_1(z_j) \quad (63)$$

$$G_2(z_j) = \frac{17017}{15912} [R(z_j)]^3 \left\{ \sigma_3(z_j) - \frac{1155}{17017} \sigma_1(z_j)\sigma_2(z_j) + \frac{50}{17017} [\sigma_1(z_j)]^3 \right\} \quad (64)$$

These quantities are given in Table II as a function of $f(z_j)$.

TABLE II

VALUES OF THE FUNCTIONS $G_1(z_j)$ AND $G_2(z_j)$ FOR USE IN EQUATION (62)

$f(z_j)$	$G_1(z_j)$	$G_2(z_j)$
0.00	1.000	1.000
.05	1.052	0.993
.10	1.150	.980
.15	1.292	.959
.20	1.484	.925
.25	1.737	.866
.30	2.065	.754
.35	2.487	.526
.40	3.032	.044
.45	3.739	-0.998
.50	4.664	-3.294
.55	5.892	-8.478
.60	7.557	-20.578
.65	9.874	-50.21
.70	13.221	-127.96
.75	18.305	-353.57
.80	26.618	-1114.9
.85	41.844	-4385.3
.875	54.96	-9954
.90	75.85	-26107
.925	113.11	-86087
.95	194.20	-430680
.975	468.44	-5915500

Equation (62) is readily solved for $f(z_j)$ with the aid of Table II after one or two successive approximations. The quantity $e^{-z_j^2}$ is obtained from $f(z_j)$ by means of tables of these functions, and C_t , computed from equation (12) as before,¹⁰ may then be substituted in equation (9) to evaluate the diffusion coefficient, D .

Integration of the Amplitude Equation for the Cell Mask

It remains to determine $g(x)$ so that disturbance of the Gouy fringes by diffraction from the masks at the ends of the cell will be minimized. Since a general treatment with unsymmetrical masking would lead to essentially the same form for $g(x)$, the notation will be simplified by considering identical masks placed symmetrically about a symmetrical diffusion boundary so $g(-x) = g(x)$, $-J_1 = J_2 = J$, and $-L_1 = L_2 = L$. Simple solutions of the amplitude equation are then obtained if it is assumed that the masks are placed

beyond the boundary, where n is essentially constant with x , and if only values of Y removed from $Y = 0$ are considered.

The contribution, $\psi_E = \psi_{E_1} + \psi_{E_2}$, to the amplitude at Y from paths E_1 and E_2 , Fig. 2, is obtained by integrating equation (2) in the form

$$\psi_E = K \int_0^\infty e^{-i[\pi j_m - \omega(L - e^{i\Omega_1 \zeta})]} (e^{i\Omega_1 d \zeta}) + K \int_{-\infty}^0 e^{i[\pi j_m - \omega(L + e^{i\Omega_2 \zeta})]} (e^{i\Omega_2 d \zeta}) \quad (65)$$

where ζ denotes the modulus about $-L$ or L and $\omega = 2\pi Y/(\lambda b)$. Since Ω_1 and Ω_2 lie between 0 and $-\pi$ this expression reduces to

$$\psi_E = -2K [\sin(\pi j_m - \omega L)]/\omega \quad (66)$$

Between $|x| = L$ and $|x| = J$ where $g(x)$ decreases from unity to zero the amplitude contribution, $\psi_M = \psi_{M_1} + \psi_{M_2}$, is

$$\psi_M = K \int_{-J}^{-L} g(x) e^{i(-\pi j_m - \omega x)} dx + K \int_L^J g(x) e^{i(\pi j_m - \omega x)} dx \quad (67)$$

or

$$\psi_M = 2K \int_L^J g(x) \cos(\pi j_m - \omega x) dx \quad (68)$$

Integrating by parts and letting $\delta = (\pi j_m - \omega x)$

$$\psi_M = 2K \left[-\frac{g(x) \sin \delta}{\omega} + \frac{g^I(x) \cos \delta}{\omega^2} + \frac{g^{II}(x) \sin \delta}{\omega^3} - \frac{g^{III}(x) \cos \delta}{\omega^4} - \frac{g^{IV}(x) \sin \delta}{\omega^5} + \dots \right]_{x=L}^{x=J} \quad (69)$$

providing the derivatives are continuous.

Neglecting the periodic function in the numerator it is seen from equation (66) that in the region $|\omega| > 1$ diffraction from a horizontal, straight-edge mask for which $g(x)$ has the form shown in Fig. 3a, is related to Y by the proportionality

$$\psi_E \propto 1/Y \quad (70)$$

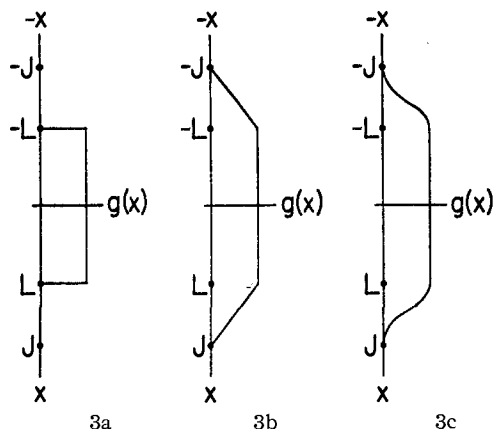


Fig. 3.—Three illustrative masking functions, $g(x)$, representing (a) horizontal straight-edge masks at $-L$ and L , (b) an improved masking function, and (c) the approximate form of the best masking function.

When $g(x)$ is linear instead of zero in the region $L < x < J$, as illustrated in Fig. 3b, the first term in ψ_M cancels ψ_E and

$$\psi_E + \psi_M \propto 1/Y^2 \quad (71)$$

This corresponds to the use of straight-edged cell masks placed at an angle to the horizontal.¹⁴ Further inspection of equation (69) indicates that diffraction from the mask may be minimized in the region below $\omega = 1$ by selecting a mask such that the first m derivatives of $g(x)$ where m is made as large as possible, are continuous between L and J and equal to zero at L and J. Figure 3c shows the approximate form of this ideal masking function. Either a variable density absorption mask or a curved, opaque, mask may be used to produce the desired form of $g(x)$.

Discussion

It is of interest to compare the expressions for fringe intensity and position derived using the Airy integral with those obtained by integrating across the saddle points. Following this comparison, which provides a test of the present development, the relations between these equations and those of the previous theory^{6,8,10} for the Gouy method will be shown. The necessity of using this extended theory in order to obtain accurate values of D when j_m is small will then be illustrated by comparing values of $e^{-z_j^2}$ obtained from this theory with those obtained from the previous theory.

Comparison of the Airy Integral and Saddle Point Expansions.—A numerical comparison of these two integration procedures is presented in Table III,

TABLE III
COMPARISON OF COMPUTED RELATIVE INTENSITIES FOR THE LOWER FRINGES OF AN IDEAL DIFFUSION

$e^{-z_j^2} = Y/C_t$	$j_m = 100$	
	$10I(Y)/(16DtK^2)$ Airy ^a	$10I(Y)/(16DtK^2)$ Saddle point ^b
1.00000	0.2483	
0.99640	.3183	
.99193	.4110	15.06
.99005	.4491	2.458
.98571	.5253	0.5632
.98324	.5558	.5209
.98059	.5732	.5291
.97775	.5698	.5339
.97473	.5382	.5134
.97151	.4722	.4630
.96812	.3724	.3640
.96454	.2479	.2441
.96079	.1218	.1203
.95685	.0275	.0273
.95275	.0016	.0016
.94847	.0629	.0629
.94403	.1918	.1918
.93941	.3215	.3214
.93463	.3624	.3624
.92969	.2676	.2676
.92459	.0965	.0967
.91934	.0003	.0003
.91393	.0847	.0847
.90837	.2595	.2594
.90267	.2935	.2935
.89682	.1210	.1210
.89083	.0002	.0002
.88470	.1395	.1393

^a Equation (22). ^b Equation (51).

which lists some computed intensities in the lower fringes formed by a Gaussian diffusion boundary. It is seen that the saddle point method, equation (51), begins to diverge as expected when $Y \rightarrow C_t$ (i.e., $e^{-z^2} \rightarrow 1$), but its agreement with the Airy integral expansion, equation (22), for this case where $j_m = 100$ is excellent for the next two fringes. If j_m is decreased the error in both calculation procedures increases, though the Airy integral method will continue to give the best results for values of Y near C_t . Further up the fringe system the situation should be reversed, with the saddle point method giving a better result than the Airy integral expansion. The intensity distribution in the "tail" of the lowest fringe, where $Y/C_t > 1$, may be computed from equation (22) while the saddle point method completely breaks down in this region.

The close relation between interference conditions (25) and (62), derived from the Airy and the saddle point expansions, respectively, will now be shown. Expanding $f(z)$, equation (11), as a power series in z and using Lagrange's method¹⁵ to invert the series gives

$$z = w \left[1 + \frac{1}{5}w^2 + \frac{31}{350}w^4 + \frac{463}{9450}w^6 + \dots \right] \quad (72)$$

where w is defined by

$$w = [(3\sqrt{\pi}/4)f(z)]^{1/3} \quad (73)$$

From equations (49) and (72) the relative downward displacement as a function of w becomes

$$Y/C_t = e^{-z^2} = 1 - w^2 + \frac{1}{10}w^4 + \frac{17}{1050}w^6 + \frac{1019}{189000}w^8 + \dots \quad (74)$$

which is similar in form to the Airy interference relation (25). To show the exact relation between the saddle point and Airy interference conditions, a series giving w^2 for intensity zeros must be obtained from equation (62), which in terms of ($j + 3/4$) becomes

$$f(z_j) = \frac{j + 3/4}{j_m} \left\{ 1 + \left(\frac{5}{72\pi^2} \right) \frac{G_1(z_j)}{(j + 3/4)^2} - \left(\frac{5}{72\pi^2} \right)^2 \left[G_1^2(z_j) + \frac{221}{30} G_2(z_j) \right] \frac{1}{(j + 3/4)^4} + \dots \right\} \quad (75)$$

By substituting

$$\rho_j = (3\pi/2)(j + 3/4) \quad (76)$$

into this expression equation (73) may be written

$$w_j^2 = \frac{\rho_j^{2/3}}{\epsilon} \left\{ 1 + \frac{5}{48} \frac{G_1(z_j)}{\rho_j^2} - \frac{5}{36} \left[\frac{35G_1^2(z_j) + 221G_2(z_j)}{256} \right] \frac{1}{\rho_j^4} + \dots \right\} \quad (77)$$

for fringe minima where ϵ is defined by equation (13). From equations (63), (64) and (72) the series expansions

$$G_1(z_j) = 1 + \frac{272}{175}w_j^4 + \frac{2096}{1125}w_j^6 + \dots \quad (78)$$

and

$$G_2(z_j) = 1 - \frac{96}{455}w_j^4 - \frac{4192}{16575}w_j^6 - \dots \quad (79)$$

are obtained which allow the following solution for w_j^2 .

TABLE IV

A COMPARISON OF REPRESENTATIVE VALUES OF $e^{-z_j^2}$ OBTAINED USING DIFFERENT EQUATIONS TO EVALUATE $f(z_j)$

	$f(z_j) = (j+3/4)/j_m^a$			$f(z_j) = Z_j/j_m^b$			$f(z_j)$ from eq. (62) ^c		
	$j_m = 100$	$j_m = 10$	$j_m = 6$	$j_m = 100$	$j_m = 10$	$j_m = 6$	$j_m = 100$	$j_m = 10$	$j_m = 6$
0	0.95393	0.78978	0.70739	0.95355	0.78821	0.70522	0.95355	0.78808	0.70476
1	.91919	.63706	.49954	.91907	.63653	.49885	.91907	.63634	.49812
2	.89106	.51751	.34112	.89098	.51724	.34075	.89098	.51699	.33969
3	.86643	.41603	.21119	.86638	.41585	.21097	.86638	.41555	.20925
4	.84402	.32703		.84399	.32690		.84399	.32651	
50	.30028			.30028			.30027		
96	.01245			.01245			.01234		
97	.00832			.00832			.00814		

^a "Quarter wave" approximation, equation (23) of ref. 10. ^b Airy integral refinement of "quarter wave" approximation, equation (11) of ref. 6. ^c Saddle point interference condition, equation (62) of this development.

$$w_j^2 = \frac{\rho_j^{2/3}}{\epsilon} \left[1 + \frac{5}{48\rho_j^2} - \frac{5}{36\rho_j^4} + \dots \right] + \frac{17}{105\epsilon^3} + \frac{131\rho_j^{2/3}}{675\epsilon^4} \left[1 + \frac{5}{48\rho_j^2} - \dots \right] + \dots \quad (80)$$

Substitution of this expression for w_j^2 into equation (74) gives the saddle point expansion for Y_j/C_t for fringe minima of an ideal diffusion, which is identical with equation (25) from the Airy integral expansion providing α_j is defined by

$$\alpha_j = -\rho_j^{2/3} \left[1 + \frac{5}{48\rho_j^2} - \frac{5}{36\rho_j^4} + \dots \right] \quad (81)$$

Since this is, in fact, the asymptotic expression for the roots of the Airy integral,¹³ equations (25) and (62) are seen to be in agreement.

Comparison with Previous Theory.—Two identical Airy integral relations for intensities in the lower fringes of Gouy patterns were derived previously by dropping higher terms in the phase difference function leaving a cubic expression with the proper slope at the origin.¹⁷ The present Airy integral development retains more terms in the expansion of the phase difference function about the origin thereby providing a refinement over the previous relations, which correspond to only the first term, $\text{Ai}(\alpha)$, of equation (22). The fringe position equation of Coulson, *et al.*,¹⁸ for the lowest intensity zero is seen to be identical with the first two terms of equation (25).

To obtain reasonable accuracy further up the fringe system quadratic or cubic expressions were used previously to fit the phase difference function at its origin and maximum,^{6,10} rather than at its origin with the correct slope. The fringe intensities¹⁹ obtained by these approximations cannot be readily compared with equations (22) and (51), but the "quarter wave" approximation for intensity zeros²⁰ which resulted from curve fitting with a quadratic is contained in the first two terms of equation (62). Furthermore, by setting $G_1(z_j)$ and $G_2(z_j)$ equal to unity instead of giving them the values in Table II, equation (62) reduces to an asymptotic series for the Airy integral refinement of the "quarter wave" approximation for intensity zeros.²¹ This correlation occurs because $f(z_j)$ must approach zero when $G_1(z_j)$ and $G_2(z_j)$ approach unity, and as $f(z_j)$ approaches zero the

cubic approximation provides an excellent representation of the actual phase difference function. Thus the present development confirms the validity of the Airy integral refinement of the "quarter wave" approximation for the lower Gouy fringes when j_m is large. Both the "quarter wave" approximation and its Airy integral refinement are seen to be precise interference conditions for the central fringes when j_m is large, since the correction terms in equation (62) become so small compared to $j + 3/4$ that they can be neglected. Close to the undeviated slit image the accuracy of both these approximate interference conditions decreases, since $G_1(z_j)$ and $G_2(z_j)$ become so large that the correction terms in equation (62) should be retained.

When j_m is small, $G_1(z_j)$ and $G_2(z_j)$ are appreciably different from unity for even the lowest fringe and the correction terms in equation (62) must be considered in determining $f(z_j)$ for every fringe. The numerical magnitudes of the errors which would otherwise be introduced are illustrated in Table IV which presents representative values of the normalized fringe displacements, $e^{-z_j^2}$, computed from the "quarter wave" approximation, the Airy integral refinement of the "quarter wave" approximation, and the saddle point interference condition (62). These values for a 6 fringe system clearly illustrate the need for using the present theory to obtain accurate values of D from experiments in which j_m is small. No value is given for the 4th fringe because the convergence of equation (62) becomes poor this far up a 6 fringe system. When j_m is increased to 10, values of $e^{-z_j^2}$ from the Airy integral refinement of the "quarter wave" approximation are seen to agree with those from equation (62) within 0.05% for fringes 0, 1 and 2. Either of these two interference conditions could therefore be used to calculate D to within 0.1% for these fringes, but equation (62) must be used to obtain this accuracy from the higher fringes.

Table IV also illustrates that for a 100 fringe system the Airy integral refinement of the "quarter wave" approximation provides values of $e^{-z_j^2}$ for the lower fringes which are in agreement with values from equation (62), but which differ slightly from those of the "quarter wave" approximation. The three interference relations are in excellent agreement for the central fringes, illustrated by the 50th fringe, but the two approximate interference conditions become slightly in error as the 96th

(17) Equation (7) of ref. 8 and equation (27) of ref. 10.
 (18) Equation (9) of ref. 8.
 (19) Equations (22) and (28) of ref. 10.
 (20) Equation (23) of ref. 10.
 (21) Equation (11) of ref. 6.

and 97th fringes are approached. It is of interest to note, however, that the positions of fringes 96 and 97 are predicted by the simple "quarter wave" approximation within the limits of the usual experimental error.

In addition to these numerical comparisons with

previous theory it should be mentioned that for the lowest fringe, $j = 0$, the Airy integral interference condition, equation (26), yields the values 0.95354, 0.78805 and 0.70474 for $e^{-z_j^2} = Y_j/C_t$ when j_m is 100, 10 and 6, respectively.

MADISON, WISCONSIN

[CONTRIBUTION FROM THE MALLINCKRODT CHEMICAL LABORATORY, HARVARD UNIVERSITY]

The Pure Quadrupole Spectra of Solid Chloroacetic Acids and Substituted Chloroacetic Acids¹

BY HARRY C. ALLEN, JR.²

RECEIVED JUNE 23, 1952

Using a frequency-modulated super-regenerative spectrometer the pure quadrupole spectrum of Cl^{35} has been measured in the chloroacetic acids and several of their derivatives. In several of these compounds multiple lines are observed, which in the case of small separations (<0.5 mc.) are attributed to crystallographically non-equivalent chlorines. In CCl_3COCl the chemically different chlorines have absorption lines separated by nearly 7 mc. A separation of slightly greater than 1 mc. in $\text{CCl}_3\text{CH}(\text{OH})_2$ is interpreted as due to intermolecular hydrogen bonding. From the variation of the chlorine frequency in the CCl_3 and CH_2Cl groups it is inferred that the electron withdrawal ability of the substituent groups measured increases in the order COO^- , CONH_2 , COCH_3 , COCH_2Cl , COOC_2H_5 , COOH .

Introduction

A nuclear electric quadrupole moment arises when the nuclear charge deviates from a spherical distribution. This permanent quadrupole moment can interact with a non-spherical extranuclear charge distribution to produce a variation in the electrostatic energy of the system with nuclear orientation. This type of effect has been observed as hyperfine structure in the rotational spectra of gas molecules and more recently the direct transitions among these energy levels have been observed in crystalline solids in the radio-frequency region of the spectrum.

In this work the pure quadrupole spectrum of chlorine³⁵ has been measured in the chloroacetic acids and several of their derivatives. These spectra are very sensitive to small changes in the gradient of the electric field at the chlorine nucleus and hence yield information concerning molecular bonding and solid state effects. It has been found that such resonance lines are influenced by different crystallographic environment³ and intermolecular bonding in the solid state,⁴ and that marked differences in the chemical bonding of a given atom give rise to rather widely separated resonance lines. It is thus possible to obtain considerable information concerning molecular bonding in the solid from a study of these spectra.

Experimental

The spectra were observed using a frequency-modulated super-regenerative spectrometer similar to that of Dean and Pound.⁵ The frequency modulation was a 30 cycles/sec. sine wave; this same frequency was applied to the horizontal plates of the display oscilloscope. A square-wave quench voltage was used, the frequencies giving the greatest sensitivity being in the region of 50–100 kc. Samples were sealed in 2-dram vials which were inserted directly in the coil which formed part of the resonant circuit of the oscillator.

(1) The research reported in this paper was supported in part by the Office of Naval Research under ONR Contract N5ori-76, Task Order V.

(2) Atomic Energy Commission Postdoctoral Fellow.

(3) H. G. Dehmelt, *Z. Physik*, **130**, 356 (1951).

(4) C. H. Townes and B. P. Dailey, *J. Chem. Phys.*, **20**, 35 (1952).

(5) C. Dean and R. V. Pound, *ibid.*, **20**, 195 (1952).

When making low temperature runs the sample and coil were immersed directly in the cooling bath.

The frequencies were measured with a war surplus frequency meter set SCR 211 AC. The frequency-meter peaks were superposed on the absorption peaks, a match being ascertained by finding the frequency-meter peak which remained superposed on the absorption peak as the quench frequency was varied. The frequency measurements are accurate to ± 5 kc. Temperatures were measured by a pentane thermometer and an iron-constantan thermocouple, both of which had been calibrated at the ice point, Dry Ice Point, and liquid nitrogen temperature. The temperature measurements are believed to be good to $\pm 1^\circ$.

Where the absorption was strong enough, the resonance due to Cl^{37} was also measured. In other cases the region was searched where the Cl^{35} resonance would be expected assuming that the observed absorption was due to Cl^{37} . The ratio of the quadrupole moments of the two isotopes, $\text{Cl}^{35}/\text{Cl}^{37}$, found from these measurements agrees within the experimental uncertainty with previously published values.^{5,6}

The CCl_3COOH used was Mallinckrodt reagent grade, the $(\text{CH}_2\text{ClCHO})_3$ was synthesized in the organic chemistry department, and the rest of the chemicals were obtained from Eastman Kodak Co. In each case the compounds were used without further purification. All samples of solid compounds were crystallized from a melt in order to ensure a maximum number of chlorine nuclei in the absorption coil. It was found necessary to age the chloral hydrate sample prepared in this way for about three months and the $(\text{CH}_2\text{ClCHO})_3$ sample for about six weeks before absorption was found.

Experimental Results

The experimental results are summarized in Table I. It should be noted that in several of the compounds multiple lines were observed. In cases where the splitting is small (<0.5 mc.) this is presumably due to crystallographically non-equivalent chlorines, while the larger separations are presumably due to differences in the chemical bonding of the chlorine atoms. Since the frequencies are temperature dependent, they have been measured from liquid nitrogen temperature up to either the melting point of the compound or room temperature, whichever is lower. The temperature dependence of the frequencies observed in the mono-chloro substituted compounds are plotted in Fig. 1.

Although CCl_3COOH is a solid at room tempera-

(6) R. Livingston, *Phys. Rev.*, **82**, 289 (1952).